

Elevated Plasma Complement Factors in *CRB1*-Associated Inherited Retinal Dystrophies

Lude Moekotte,¹ Joke H. de Boer,¹ Sanne Hiddingh,¹ Aafke de Ligt,¹ Xuan-Thanh-An Nguyen,² Carel B. Hoyng,³ Chris F. Inglehearn,⁴ Martin McKibbin,^{4,5} Tina M. Lamey,⁶ Jennifer A. Thompson,⁷ Fred K. Chen,^{6,7} Terri L. McLaren,^{6,7} Alaa AlTalbish,⁸ Daan M. Panneman,⁹ Erica G. M. Boonen,⁹ Sandro Banfi,^{10,11} Béatrice Bocquet,^{12,13} Isabelle Meunier,^{12,13} Elfride De Baere,^{14,15} Robert Koenekoop,^{16,17} Monika Ołdak,¹⁸ Carlo Rivolta,^{19–21} Lisa Roberts,²² Raj Ramesar,²² Rasa Strupaitė-Šileikienė,²³ Susanne Kohl,²⁴ G. Jane Farrar,²⁵ Marion van Vugt,²⁶ Jessica van Setten,²⁶ Susanne Roosing,⁹ L. Ingeborgh van den Born,²⁷ Camiel J. F. Boon,^{2,28} Maria M. van Genderen,^{1,29} and Jonas J. W. Kuiper¹

¹Department of Ophthalmology, University Medical Center Utrecht, Utrecht, the Netherlands

²Department of Ophthalmology, Leiden University Medical Center, Leiden, the Netherlands

³Department of Ophthalmology, Radboud University Medical Center, Nijmegen, the Netherlands

⁴Division of Molecular Medicine, Leeds Institute of Medical Research, University of Leeds, Leeds, United Kingdom

⁵Department of Ophthalmology, St. James's University Hospital, Leeds, United Kingdom

⁶Centre for Ophthalmology and Visual Science, The University of Western Australia, Perth, Western Australia, Australia

⁷Australian Inherited Retinal Disease Registry & DNA Bank, Department of Medical Technology and Physics, Sir Charles Gairdner Hospital, Nedlands, Western Australia, Australia

⁸St. John of Jerusalem Eye Hospital Group, East Jerusalem, Palestine

⁹Department of Human Genetics, Radboud University Medical Center, Nijmegen, the Netherlands

¹⁰Telethon Institute of Genetics and Medicine, Pozzuoli, Italy

¹¹Department of Precision Medicine, University of Campania "Luigi Vanvitelli", Naples, Italy

¹²Institute for Neurosciences of Montpellier (INM), University of Montpellier, INSERM, Montpellier, France

¹³National Reference Center for Inherited Sensory Diseases, University of Montpellier, CHU, Montpellier, France

¹⁴Department of Biomolecular Medicine, Ghent University, Ghent, Belgium

¹⁵Center for Medical Genetics, Ghent University Hospital, Ghent, Belgium

¹⁶McGill University Health Center (MUHC) Research Institute, Montreal, QC, Canada

¹⁷Departments of Paediatric Surgery, Human Genetics, and Adult Ophthalmology, McGill University Health Center, Montreal, QC, Canada

¹⁸Department of Histology and Embryology, Medical University of Warsaw, Warsaw, Poland

¹⁹Institute of Molecular and Clinical Ophthalmology Basel, Basel, Switzerland

²⁰Department of Ophthalmology, University of Basel, Basel, Switzerland

²¹Department of Genetics and Genome Biology, University of Leicester, Leicester, United Kingdom

²²UCT/MRC Precision and Genomic Medicine Research Unit, Division of Human Genetics, Department of Pathology, Institute of Infectious Disease and Molecular Medicine, Faculty of Health Sciences, University of Cape Town, Cape Town, South Africa

²³Center of Eye Diseases, Clinic of Ear, Nose, Throat, and Eye Diseases, Institute of Clinical Medicine, Faculty of Medicine, Vilnius University, Vilnius, Lithuania

²⁴Institute for Ophthalmic Research, Centre for Ophthalmology, University of Tübingen, Tübingen, Germany

²⁵The School of Genetics & Microbiology, The University of Dublin Trinity College, Dublin, Ireland

²⁶Department of Cardiology, University Medical Center Utrecht, Utrecht, the Netherlands

²⁷Het Oogziekenhuis Rotterdam, Rotterdam, the Netherlands

²⁸Department of Ophthalmology, Amsterdam UMC, Amsterdam, the Netherlands

²⁹Bartiméus, Diagnostic Centre for complex visual disorders, Zeist, the Netherlands

Correspondence: Lude Moekotte,
Heidelberglaan 100, 3584 CX
Utrecht, the Netherlands;
l.moekotte@umcutrecht.nl.

PURPOSE. To determine the profile of inflammation-related proteins and complement system factors in the plasma of *CRB1*-associated inherited retinal dystrophies (*CRB1*-IRDs).

METHODS. We used the Olink Explore 384 Inflammation II panel for targeted proteomics in 30 cases and 29 controls (cohort I) to identify immune pathways involved in *CRB1*-IRDs. Genotyping was performed in cohort I and a second cohort of 123 patients from 14 countries and 1292 controls (cohort II).

Received: March 21, 2024

Accepted: September 3, 2024

Published: February 21, 2025

Citation: Moekotte L, de Boer JH, Hiddingh S, et al. Elevated plasma complement factors in *CRB1*-associated inherited retinal dystrophies. *Invest Ophthalmol Vis Sci*. 2025;66(2):55. <https://doi.org/10.1167/iovs.66.2.55>

RESULTS. A significant shift in complement cascade factors was observed in plasma proteomes of *CRB1*-IRD patients (enrichment for complement cascade, $P_{adj} = 3.03 \times 10^{-15}$). We detected higher plasma levels of complement factor I and complement factor H [CFH] ($q = 0.008$ and $q = 0.046$, respectively, adjusted for age and sex), inhibitors of complement component 3 (C3), which correlated significantly (Pearson's coefficient >0.6) with elevated levels of C3 ($q = 0.064$). The *CRB1* missense variants frequently found in patients showed a strong linkage disequilibrium with the common *CFH* variant rs7535263 ($D' = 0.97$ for p.(Cys948Tyr); $D' = 1.0$ for p.(Arg764Cys)), known to be linked with altered plasma CFH-related protein levels. Correction for the *CFH* genotype revealed significantly elevated plasma levels of CFH-related 2 (CFHR2) in *CRB1*-IRD patients ($q = 0.041$).

CONCLUSIONS. *CRB1*-IRDs are characterized by changes in plasma levels of complement factors and proteins of the innate immune system, and linkage between *CRB1* and *CFH* genes implicates functional variants of the *CFH*-*CFHR* locus with specific pathogenic variants of *CRB1*.

Keywords: inherited retinal dystrophy, *CRB1*, proteomics, complement, *CFH*, inflammation

The *Crumbs homolog 1* (*CRB1*) gene (also known as *RP12*) is a transmembrane protein that functions in the integrity preservation of the photoreceptor layer of the retina. *CRB1* pathogenic variants cause a spectrum of rare autosomal recessive inherited retinal dystrophies (*CRB1*-IRDs) characterized by photoreceptor cell death and early visual impairment.^{1–3} There are many pathogenic variants associated with *CRB1*-IRDs, and the clinical phenotypes vary considerably in the severity of disease.^{1,3} Although some correlation between *CRB1* genotype and clinical phenotypes can be found,⁴ overall, there is surprisingly little genotype–phenotype correlation, even among cases with identical pathogenic variants.^{1,3} Therefore, it has been hypothesized that phenotypic variation among patients may be caused by factors other than the underlying *CRB1* pathogenic variants.¹

The presence of vitreous inflammation or cystoid macular edema in some patients with *CRB1*-IRDs suggests that inflammatory pathways may be involved in the pathophysiology.^{5,6} Indeed, inflammatory genes and complement factors are upregulated in the retinas of rd8 mice homozygous for a *Crb1* gene pathogenic variant.^{1,5–9} Furthermore, we previously showed that patients with *CRB1*-IRDs exhibit changes in their peripheral blood T cells and dendritic cells.^{6,10} These findings suggest that variability of immune responses between patients may contribute to differential clinical phenotypes, but there have been few studies that examine the immune profiles of *CRB1*-IRD patients.^{6,10}

A way to study immune profiles is by examining blood proteins, which contribute to immune responses and function by modifying the signaling of cytokines, triggering acute-phase reactions, and activating complement cascades. Targeted proteomics allows the accurate quantification of hundreds of blood proteins in patient samples to determine, in depth, the immune profile of disease and identify disease-related mechanisms.¹¹ This technique has provided insight into the blood proteome of diverse eye conditions such as age-related macular degeneration (AMD), retinopathy of prematurity, uveitis, uveal melanoma, and diabetic retinopathy.^{12–18} The genetic variant rs7535263 in *CFH* is located adjacent to the *CRB1* gene on chromosome 1, has been shown to strongly correlate with the levels of complement factor H-related proteins, and is genetically associated with several other diseases of the retina.^{19–26} This suggests that this variant could be significant in quantitative analysis of plasma complement factors.

In this study, we conducted targeted 370-plex proteomics of blood plasma proteins in *CRB1*-IRD patients and healthy controls to determine the plasma concentrations of inflammation-related proteins. In the same cohort and in a validation cohort, we determined the *CFH* gene variant rs7535263 to test for associations between protein expression and genotype.

METHODS

Patients

This study was performed in compliance with the guidelines of the Declaration of Helsinki and has the approval of the local Institutional Review Board (University Medical Center Utrecht [UMCU]). In total, 30 patients were referred to the UMCU from the Amsterdam University Medical Centers, Leiden University Medical Center, Bartiméus Diagnostic Center for complex visual disorders, The Rotterdam Eye Hospital and Rotterdam Ophthalmic Institute, and Groningen University Medical Center for recruitment at the outpatient clinic of the Department of Ophthalmology of the UMCU (MEC-14-065). Each patient provided written informed consent before participation and blood collection. The *CRB1*-IRD diagnosis was established by ophthalmic examination, imaging, full-field electroretinography, and next-generation sequencing or whole-exome sequencing. Patients were considered to have a molecularly confirmed *CRB1*-IRD when they harbored two or more rare functional variants (i.e., disease-causing *CRB1* variants, such as missense, deletions, loss of function, or splice altering variants) affecting both gene copies of *CRB1* (Supplementary Table S1).

We excluded patients with systemic inflammatory conditions at the time of sampling and/or patients who had received systemic immunomodulatory treatment. On the day of inclusion, patients were examined by visual acuity measurement, and an experienced uveitis specialist performed slit-lamp examination to assess vitreous cells and vitreous haze.

Next, we obtained blood from 29 anonymous age-matched healthy blood bank donors with no history of ocular inflammatory disease who gave broad written informed consent at the research blood bank of the University Medical Center Utrecht (The “Mini Donor Dienst”).

Targeted Blood Proteomics

Venous blood samples were collected in EDTA Lavender Top Tubes (#362084; BD Biosciences, Franklin Lakes, USA) and then centrifuged for 10 minutes ($400 \times g$) within an hour of blood collection (Supplementary Table S2). Plasma was transferred to a Falcon 15 mL Conical Centrifuge Tube (Corning Inc., New York, USA) and centrifuged for 10 minutes ($1500 \times g$), after which the cleared plasma was transferred and stored in Micronic 1.4-mL round-bottom tubes (#MP32022; Micronic, Lelystad, the Netherlands) at -80°C . For proteomic analysis of plasma, patient and control samples were randomized over three 96-well plates (#72.1980; Sarstedt, Nümbrecht, Germany) and sealed (#232698; Thermo Fisher, Waltham, MA, USA) before shipment on dry ice to the Olink Proteomic facility at the Erasmus Medical Center, Rotterdam, the Netherlands. We used the Olink Explore 384 Inflammation II panel for targeted proteomics of blood plasma. This Olink technology is based on proximity extension assays coupled with next-generation sequencing (NGS) and is capable of the simultaneous relative quantification of 370 protein analytes.⁷

TaqMan Single-Nucleotide Polymorphism Genotyping

Genomic DNA of 59 peripheral mononuclear blood samples in an RLT Plus lysis buffer (#1053393; Qiagen, Hilden, Germany) was isolated with the AllPrep DNA/RNA/miRNA Universal Kit (#80224; Qiagen). Next, we determined the rs7535263 variant with the TaqMan single-nucleotide polymorphism (SNP) genotyping technology (#4351379; Thermo Fisher). Genotypes were called using QuantStudio 12K Flex software (Thermo Fisher). Linkage disequilibrium (r^2 or D') data for rs7535263 in the CEU population of the 1000 genomes were obtained with the LDproxy tool with genome build *GRCh37* in *LDlink*.²⁷ The estimated recombination rate for Utah residents with Northern and Western European ancestry CEU (Utah residents (CEPH) with Northern and Western European ancestry, build *GRCh37*) generated by Adam Auton was obtained via the 1000 Genomes ftp site (ftp://ftp.1000genomes.ebi.ac.uk/vol1/ftp/technical/working/20130507_omni_recombination_rates/).²⁸ Using phased whole-genome sequencing data of $\sim 150,000$ individuals of the UK Biobank (UKB), we calculated the linkage disequilibrium (LD) between rs7535263 in *CFH* and *CRB1* missense variants p.(Cys948Tyr) and p.(Arg764Cys), using the *-ld* function in *plink* 2.0.^{29,30} These are two relatively more commonly found *CRB1* missense variants with allele frequencies in the UKB that permit meaningful LD calculations (i.e., others are too rare).^{29,30} The UKB has ethical approval from North West–Haydock Research Ethics Committee (REC reference: 16/NW/0274). Details of the UK Biobank study have been described in detail previously.³¹ This research has been conducted using the UK Biobank Resource under Application Number 24711.

TaqMan genotyping of rs7535263 was also performed in an independent validation cohort (cohort II) of 123 *CRB1*-IRD patients from the United Kingdom, Australia, Palestine, Italy, France, Belgium, the Netherlands, Canada, Poland, Switzerland, South Africa, Lithuania, Germany, and Ireland (MEC-2010-359) and 1292 Dutch controls from the amyotrophic lateral sclerosis study.³² All patients provided written informed consent for genetic testing at the center of recruitment. *CRB1*-associated genetic diagnoses were made by targeted gene Sanger sequencing or established

recently through a sequencing panel for retinitis pigmentosa and Leber congenital amaurosis using a single-molecule molecular inversion probes (smMIP) method.³³ TaqMan SNP genotyping (#4351379; Thermo Fisher) was performed on genomic DNA following the same procedure as described above by the laboratory of the Department of Human Genetics, Radboud University Medical Center, Nijmegen, the Netherlands.

Statistical Analyses

Proteome analyses were performed on Normalized Protein eXpression (NPX) units from the output of the Olink analysis in R and RStudio (version 4.2.2) using the Olink Analyze R package.³⁴ One protein, TNFSF9, had 13 missing data points, and 10 proteins did not pass quality control (Olink assay report). These proteins were removed before group analyses. The *prcomp* function of R base was used to perform principal component analysis (PCA). Differential expression analysis was performed using a likelihood ratio test (LRT) with age and sex as covariates in the models, and we used the *qvalue* package from Bioconductor to correct *P* values for multiple testing.³⁵ Overrepresentation analysis (or enrichment) was performed on proteins with nominal significant differential expression levels ($P < 0.05$) with the *ClusterProfiler* R package and using the WikiPathways database as a reference.³⁶ The results were plotted using the *dotplot* function of the *enrichplot* R package, and the *P* values from enrichment analysis were adjusted with the Benjamini–Hochberg (BH) procedure, using the *p.adjust* function in R base, and *P* values (*P*_{adj}) < 0.05 were considered statistically significant.³⁷ Disease association for rs7535263 was assessed with *Plink* using Fisher's exact test and expressed as the odds ratio (OR) with a 95% confidence interval (CI). We performed an LRT to assess the relation between the genotype and the protein expression levels and visualized the results using the *corrplot* R package.³⁸ Other figures were generated with the *ggplot2* package.³⁹ The explained variance (R^2) by the genotype of rs7535263 of plasma proteins was calculated using the squared Pearson correlation coefficient (r^2) using the *cor* function in R base.

RESULTS

Generation of a High-Quality Plasma Proteome of *CRB1*-IRD Patients

To explore the composition of inflammatory mediators in the plasma proteome of *CRB1*-IRD patients, we conducted 370-plex targeted proteomics using proximity extension assays combined with NGS in a cohort of 30 patients and 29 healthy controls. To ensure high-quality data for quantitative proteomic analysis, we first applied a stringent quality control process. We first filtered out low-quality analytes by removing proximity extension assays that did not pass quality control in all plasma samples, resulting in 358 (97%) proteins that passed this filtering step. We detected no outlier plasma samples as shown by the relatively comparable sample median and sample interquartile range as well as NPX (the protein expression unit, which is in \log_2 scale) distribution between plasma samples (Figs. 1A, 1B). However, nine plasma samples exhibited internal controls deviating >0.3 NPX from the plate median, which were also removed from the data set (Fig. 1B). PCA on the 50 remaining plasma samples revealed a moderate plate effect that

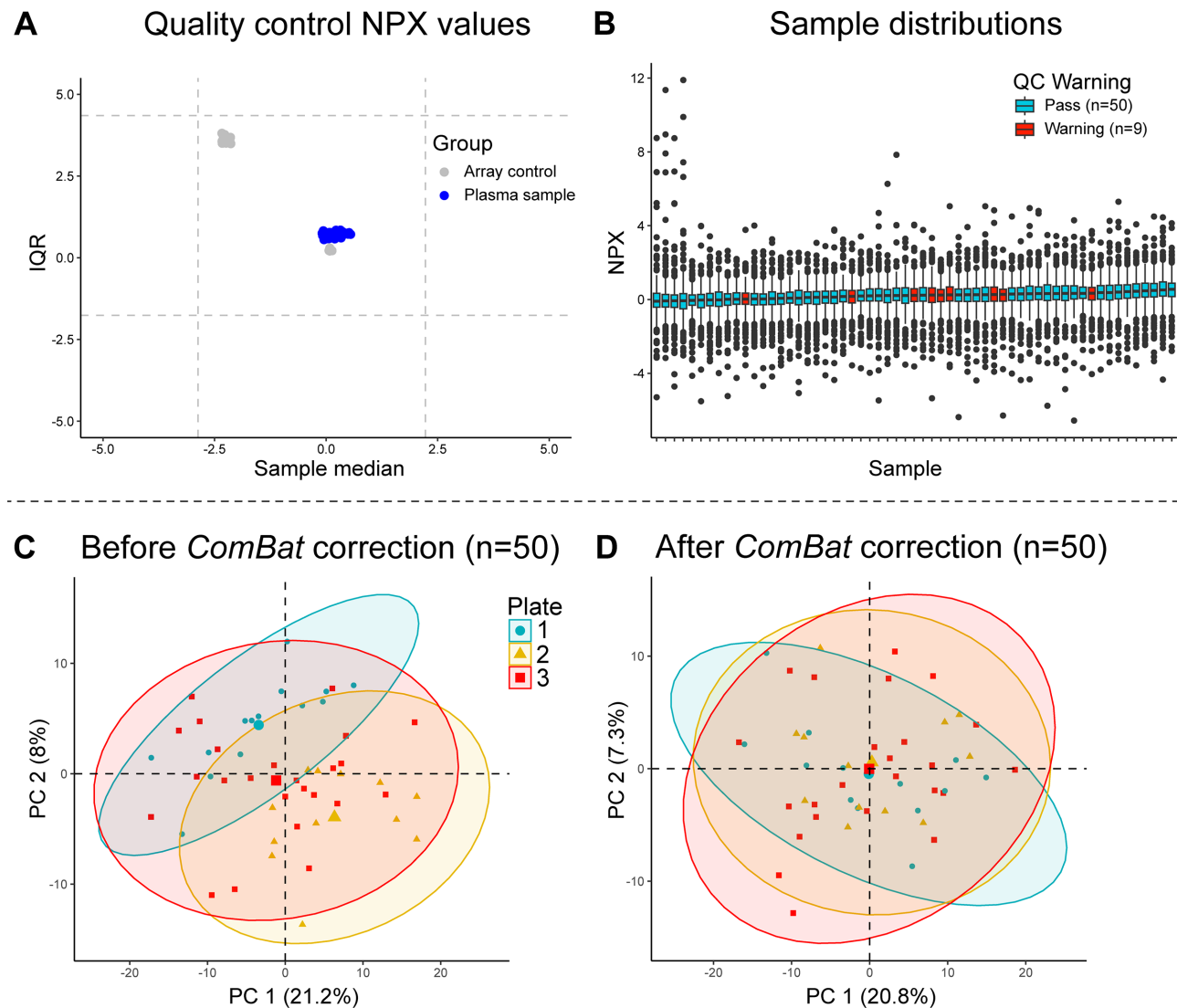


FIGURE 1. Quality control of plasma proteomic profiling by proximity extension assays combined with NGS. **(A)** The median and the interquartile range (IQR) of the distribution of NPX values for each of 59 plasma samples (blue) measured in this study and internal plate and array controls (gray). The horizontal and vertical dashed lines indicate ± 2.5 standard deviations of all sample medians (x-axis) and IQRs (y-axis). **(B)** The sample-wise distributions of NPX values for the Inflammation II panel. Boxplots of NPX values for each plasma sample are along the x-axis and NPX values along the y-axis. The center line represents the median. Plasma samples are colored by “QC_Warning” (Warning = >0.3 NPX from the median value of all samples on the plate). **(C, D)** The first two principal components of 50 plasma samples and 359 proteins before and after batch correction with *Combat*.

we mitigated by using the *Combat* algorithm to account for batch effects (Figs. 1C, 1D). As a result, a high-quality proteomic data set was generated for downstream analysis.

Elevated Concentrations of Plasma Complement Factors in *CRB1*-IRD Patients

We then compared the plasma proteome of patients to controls using linear models that include age and sex (likelihood ratio test). At a false discovery rate of 5% ($q < 0.05$), we detected 10 proteins with significantly different abundance between patients and controls (Fig. 2A and Supplementary Table S3). Among these, elevated levels were observed for complement factor I (CFI), complement factor H (CFH), protein S (PROS1), serpin family D member 1 (SERPIND1), and a disintegrin-like and metalloproteinase with thrombospondin type 1 (ADAMTS1) in patients compared to healthy controls (Fig. 2B). We also

detected significantly decreased levels for serine protease 22 (PRSS22) and microfibrillar-associated protein 4 (MFAP4) in *CRB1*-IRD patients.

The 62 proteins most associated with *CRB1*-IRD patients (nominal $P < 0.05$) showed overall considerable positive correlation in expression levels, with close clustering of CFI, CFH, C3, and SERPIND1 (Fig. 2C). These 62 proteins were strongly enriched for pathways involving platelet biology, the complement system, and coagulation cascades (Fig. 2D and Supplementary Table S4). In detail, the most enriched pathway was the “Complement cascade” (e.g., *Reactome* pathway R-HSA-166658, $\text{Padj} = P = 3.03 \times 10^{-15}$, Fig. 2D). In total, 12/62 *CRB1*-IRD associated proteins were linked to this pathway, including the significantly elevated proteins CFH, CFI, and PROS1. In addition, PROS1 and SERPIND1 were also linked to coagulation pathways (i.e., “Formation of Fibrin Clot (Clotting Cascade),” $\text{Padj} = P = 4.69 \times 10^{-7}$). Another enriched pathway included the “Extracellu-

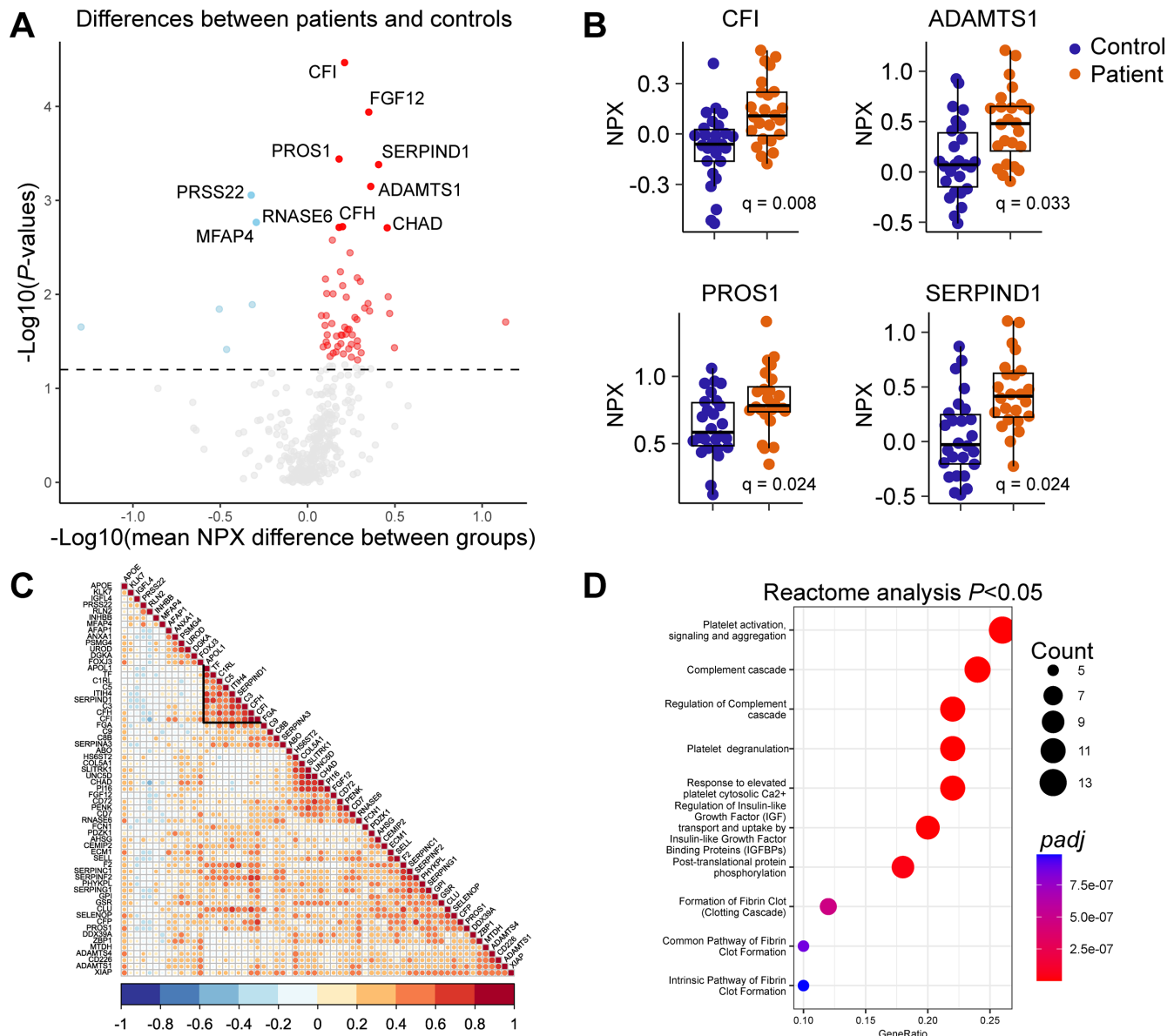


FIGURE 2. Plasma complement and coagulation proteins are associated with *CRB1*-IRDs. (A) Volcano plot showing the $-\log_{10}(P\text{ values})$ versus the $\log_2(\text{mean NPX difference between groups})$ in plasma protein concentrations. Red indicates proteins with a significant increase in protein concentration, and blue indicates proteins with a significant decrease in protein concentration in patients compared to controls. The dotted line indicates $P < 0.05$. (B) Scatterplots of the levels of CFI, ADAMTS1, PROS1, and SERPIND1 in the plasma of patients (orange) and controls (blue). The median and the interquartile range (IQR) of the distribution of NPX values for each plasma sample are shown. (C) Correlation plot of the 62 proteins most associated with *CRB1*-IRDs ($P < 0.05$ from differential expression analysis). Red indicates a positive correlation, white indicates no correlation, and blue indicates a negative correlation between plasma protein analytes. (D) Dot plot showing the top 10 results from enrichment analysis using the plasma proteins associated with *CRB1*-IRDs, as shown in C.

lar matrix organization" (R-HSA-1474244, $P_{adj} = P = 5.84 \times 10^{-3}$) based on the significantly altered plasma proteins ADAMTS1 and MFAP4 (Supplementary Table S4). Collectively, these results show that elevated levels of complement factors and inflammation-related proteins characterized the plasma proteome of patients with *CRB1*-IRDs.

The *CFH* Genotype Is Altered in Dutch *CRB1*-IRD Patients

On chromosome 1, the *CRB1* gene is located adjacent to the *CFH*-*CFHR* locus, which is implicated in other retinal conditions by influencing plasma complement protein levels and

other proteins detected in our study. Therefore, we hypothesized that linkage between *CRB1* and the *CFH*-*CFHR* locus could influence the plasma proteome of *CRB1*-IRD patients. To investigate this, we genotyped the common intronic SNP rs7535263 (LD $r^2 = 1.0$ with AMD risk variant rs1410996 in the CEU population of the 1000 Genomes). The genotype of rs7535263 was shown to have the strongest correlation with the gene expression levels of *CFH*-related 1 to 4 (*CFHR1*–4) in the Genotype-Tissue Expression project and is associated with multiple retinal diseases (e.g., AMD, multifocal choroiditis, and serious chorioretinopathy), as well as with other immune mediators on our array, such as CFP.^{19–26}

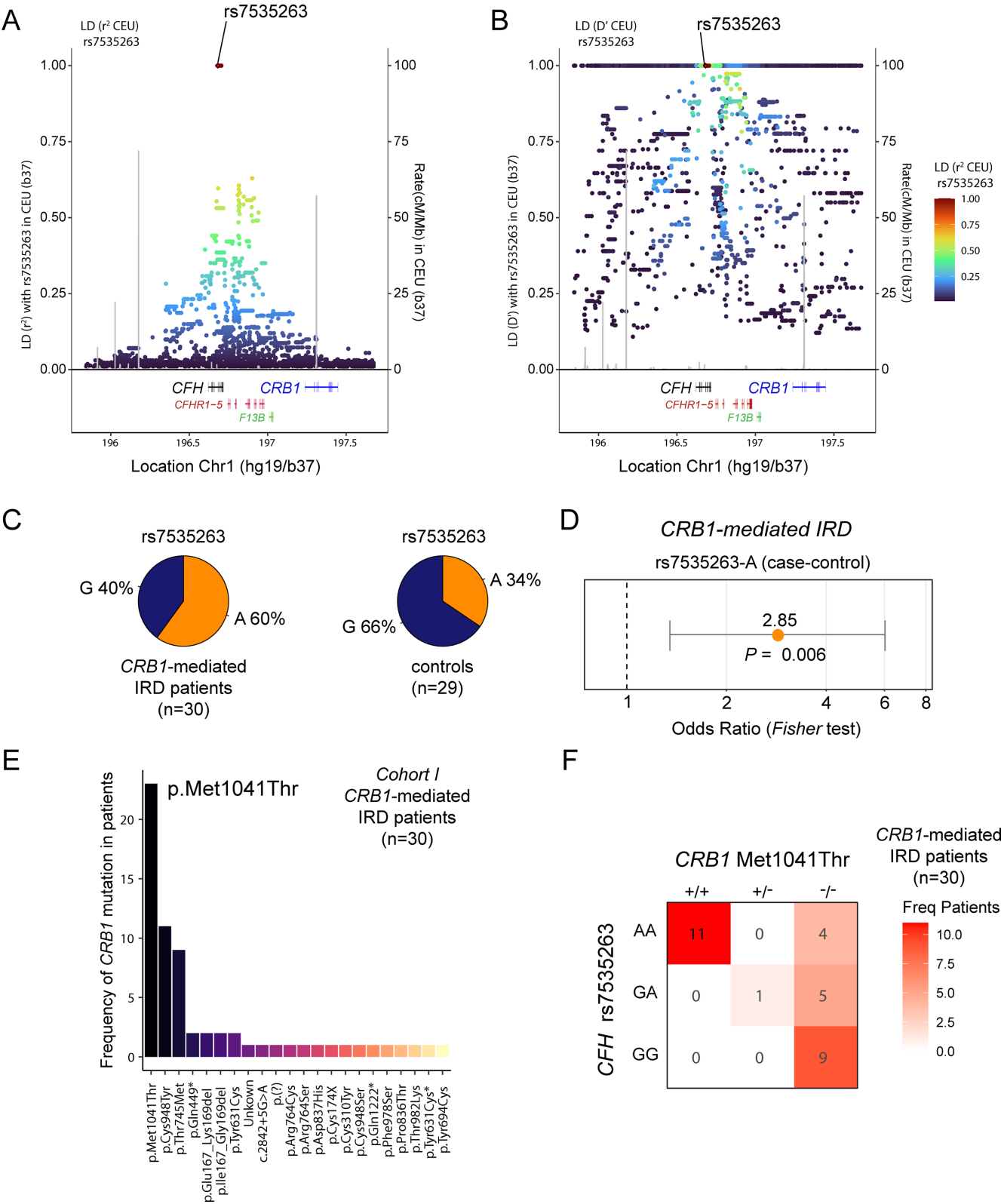


FIGURE 3. Skewed allelic distribution for a common *CFH* variant in patients with *CRB1*-IRDs. (**A**, **B**) Linkage disequilibrium (r^2 metric, *left*; D' metric, *right*) for rs7535263 in the CEU superpopulation of the 1000 Genomes Project. Genes in the *CFH* extended locus and *CRB1* are highlighted. (**C**) Allele frequency distribution for rs7535263 in cohort 1 in cases and controls. (**D**) The odds ratio, 95% confidence interval, and P value from Fisher's exact test for the A allele of rs7535263 in case-control analysis of cohort 1. (**E**) The frequency of each *CRB1* pathogenic variant in cohort 1. (**F**) Heatmap of the frequency of patients with rs7535263 genotype and *CRB1* Met1041Thr variant dosage in cohort 1.

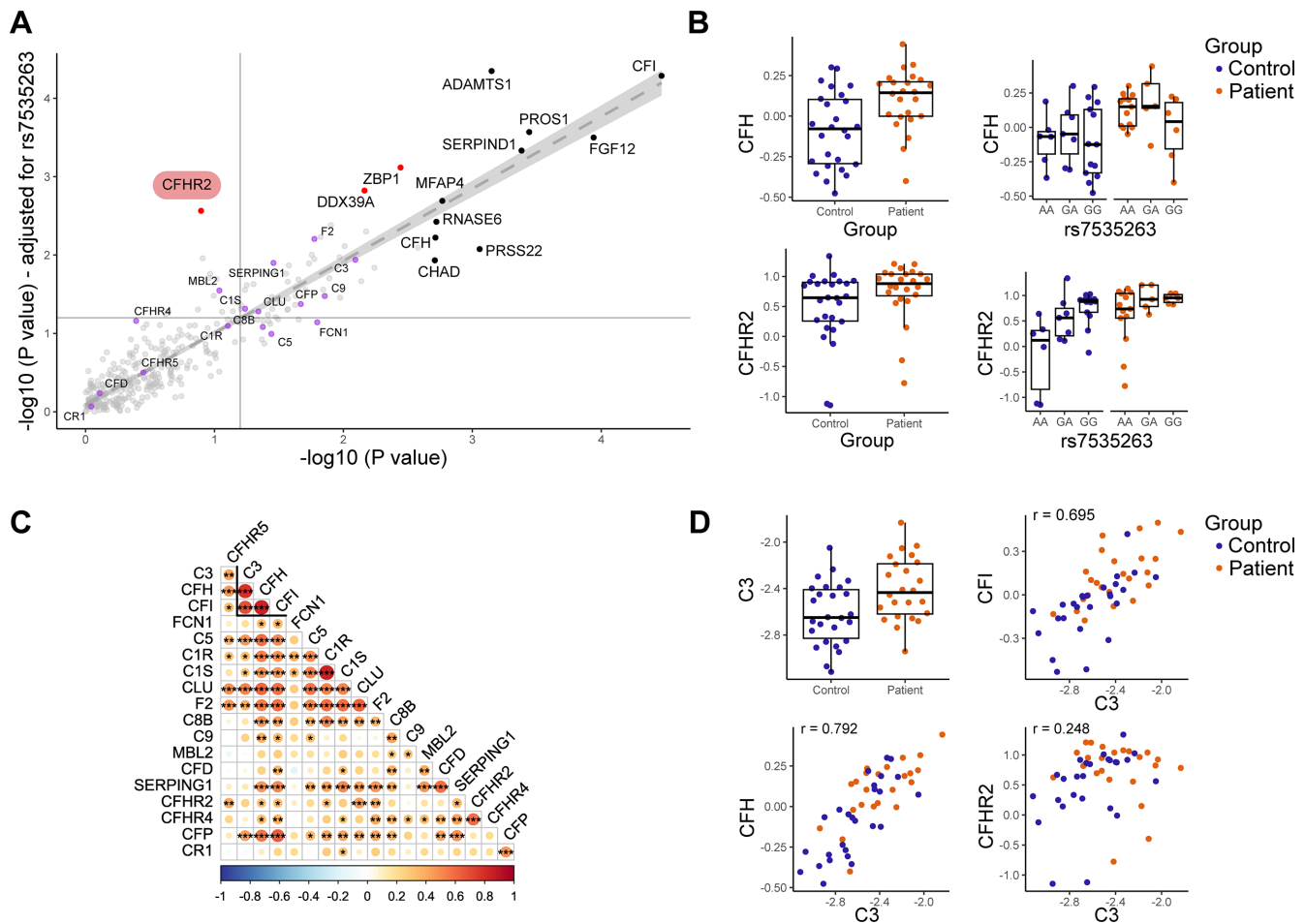


FIGURE 4. Elevated CFI and CFH levels correlate with plasma C3 in *CRB1*-IRDs. **(A)** Results from differential expression analysis before (x-axis) and after (y-axis) corrected for the genotype of rs7535263. The $-\log_{10}(P \text{ value})$ for each protein analyte is shown. *Red* indicates proteins that became statistically significantly different between cases and controls after adjusting for the genotype of rs7535263, and *black* indicates the 10 significant plasma proteins ($q < 0.05$) in our initial group comparison. *Purple* highlights plasma proteins involved in complement pathways. The *dotted line* indicates $P < 0.05$. **(B)** Boxplots show the levels of CFH and CFHR2 in cases and controls in bulk and stratified by the genotype of *CFH* variant rs7535263. **(C)** Correlation plot of the 18 proteins involved in complement pathways. *Red* indicates a positive correlation, *white* indicates no correlation, and *blue* indicates a negative correlation between plasma protein analytes. **(D)** Boxplot and correlation plots of the levels of CFI, CFH, CFHR2, and C3 in plasma in patients (*orange*) and controls (*blue*).

The LD signatures of rs7535263 (r^2 and D' with linked SNPs) and genetic recombination rates support that *CRB1* variants and *CFH*-*CFHR* variants may reside in the same haplotype block (Figs. 3A, 3B). As expected, the allele frequency of rs7535263 of Dutch controls (A allele of rs7535263 = 0.34) was similar to that of the comparable North European populations of the 1000 genomes (0.36 in GBR [British in England and Scotland] population). In contrast, the A allele of *CFH*-rs7535263 was significantly higher in patients compared to controls (A allele of rs7535263; OR = 2.85; 95% CI, 1.35–6.02; $P = 6.19 \times 10^{-3}$) (Figs. 3C, 3D). The most common *CRB1* variant in our cohort was the homozygous p.(Met1041Thr) missense variants (*CRB1* c.3122T > C; p.(Met1041Thr)) found in 11 of 30 patients (37% of patients), which has been previously linked to a large consanguineous pedigree originating from a genetically isolated population in the Netherlands (Figs. 3E, 3F). While this variant is rare in the general European population (allele frequency = 0.00001 for rs62635656 in the gnomAD database), the variant is found to be relatively more common (>1%) in this specific geographical

Dutch area (Supplementary Table S1).⁴⁰ We suspected that this deviation in allele frequency may therefore be the result of biological relatedness among cases (i.e., founder effect). All patients in our cohort homozygous for p.(Met1041Thr) were also homozygous for the A allele of rs7535263, which results in an excess of homozygotes for the A allele of the *CFH* variant rs7535263 and provides circumstantial evidence that biological relatedness between cases may likely influence our analysis of plasma complement factors. In a validation cohort of 123 *CRB1*-IRD cases from multiple countries and 1292 Dutch control participants, the A allele of rs7535263 was not significantly more frequent in patients compared to controls (A allele of rs7535263; OR = 1.24; 95% CI, 0.95–1.61; $P = 0.12$). However, similar to the first cohort, a skewed allele frequency was observed for rs7535263 specifically in relation to the most common *CRB1* variant, p.(Cys948Tyr). This variant is also a common *CRB1* variant in previous reports,⁴¹ indicating possible linkage disequilibrium between specific variants of *CRB1* and *CFH*. Utilizing data from large population databases such as the UKB may allow more accurate LD calculation between rare

missense variants in *CRB1* and rs7535263 in the *CFH* gene. To this end, we used phased whole-genome sequencing data from the UKB from ~150,000 individuals and calculated LD for *CRB1* missense variants. Two *CRB1* missense variants commonly found in *CRB1*-IRD cases with UKB allele frequencies that allow meaningful LD calculations (allele frequency >0.0001) display strong LD with rs7535263 in *CFH*⁴²; the p.(Cys948Tyr) variant is in LD with the G allele of rs7535263 ($D' = 0.97$, UKB), and the p.(Arg764Cys) variant is in full LD ($D' = 1.0$ in UKB) with the A allele of rs7535263. Collectively, these results confirm our initial observation that patients with *CRB1* missense variants may coinherit functional variants in the adjacent *CFH* locus, which should be considered in quantitative analysis of plasma complement factors in *CRB1*-IRD patients.

***CRB1*-IRD Patients Show Elevated Plasma CFHR2 After Adjusting for the *CFH* Genotype**

We investigated the effect of rs7535263 on the plasma concentrations of immune mediators in healthy controls. In line with previous studies, the genotype of rs7535263 explained a significant proportion of the plasma levels of several proteins encoded by genes in the extended *CFH*-*CFHR* locus, including CFH-related protein 2 (CFHR2) ($R^2 = 0.36$) and CFHR4 ($R^2 = 0.24$), but not CFH ($R^2 = 0.003$) (Supplementary Table S5 with R^2 values), indicating that the genotype of this SNP may interfere with our analysis of some proteins in *CRB1* patients. We therefore repeated our proteomic analysis for cohort 1 while correcting for the genotype of rs7535263 (along with sex and age). This analysis revealed that the association with the 10 significantly altered plasma proteins ($q < 0.05$) in our initial group comparison was not significantly influenced by the genotype, such as CFI ($q_{rs7535263} = 0.003$) and CFH ($q_{rs7535263} = 0.06$) (Figs. 4A, 4B and Supplementary Table S3), and all 10 remained within a false discovery rate of 7% ($q < 0.07$). However, adjusting for rs7535263 revealed additional proteins associated with *CRB1*-IRDs, most likely by improving statistical power by reducing residual variance. Among these plasma proteins was CFHR2 ($q_{rs7535263} = 0.04$), further supporting dysregulation of complement pathways in *CRB1*-IRDs (Figs. 4A, 4B). Correcting for rs7535263 also revealed a significant association ($q_{rs7535263} < 0.05$) with the DNA binding protein ZBP1, and RNA helicase DDX39A, which was previously also associated with the genotype of rs7535263 in multifocal choroiditis patients.²⁴

The identified complement factors CFI, CFH, and CFHR2 all target C3,^{43,44} an important downstream effector of the complement system, which was also increased in *CRB1*-IRD patients, albeit at nominal significance ($q = 0.064$) (Fig. 4D). Based on the profile of complement factors in our array ($n = 18$), we performed a correlation analysis to identify the factors associated with plasma C3 levels in our cohort. This analysis revealed that CFH and CFI, but not CFHR2, strongly correlated with the levels of plasma C3 (Figs. 4C, 4D).

DISCUSSION

In this study, we examined the plasma proteome of patients with *CRB1*-IRDs, whose levels of inflammation-related proteins and complement factors were notably elevated compared to healthy controls. A remarkable observation was the detection of elevated CFH and CFHR2 proteins in *CRB1*-

IRDs, which is interesting because elevated plasma levels of CFHR2 have been linked with other eye conditions, including AMD and multifocal choroiditis patients.^{12,19,20,24,45} CFH/CFHR proteins are all involved in the regulation of the complement component C3,^{44,46} which was supported by our observation of a strong correlation between CFI and CFH with C3 in plasma. Elevated CFH/CFHR proteins may be a response to increased levels of C3, a compensatory mechanism in order to reduce complement activation. Our results are also in line with animal models of IRDs (rd10 mice), which show an increase in C3 protein levels and C3 activation, as well as an increase of mRNA of *Cfb* and *Cfi* in the retina.⁴⁷ While C3 is important for complement activation and can cause microglial activation and photoreceptor cell injury,⁴⁸ it has also been shown to mediate retina-protective signaling in other murine models of retinal degeneration but will require human trials with (intravitreal) anti-C3 therapy to elucidate its potential as a therapeutic target for *CRB1*-IRDs.^{47,49,50} However, our study did not measure complement activation markers directly but rather essential complement components. Increased levels of essential complement components do not necessarily indicate increased activation, as depletion could also reflect activation through increased cleavage. Additionally, targeted proteomics, while powerful, has inherent (selection) bias and limited coverage. The panel we have used, however, provides an extensive panel of proteins related to inflammation. Regardless, the increased levels of complement factors and inflammation-related proteins that we found in patients support immune-mediated pathways involved in *CRB1*-IRDs.

Recent research with models of *CRB1*-associated inherited retinal dystrophy shows that a “leaky gut,” or increased gut permeability, may play a role in *CRB1*-IRDs.⁵¹ Bacterial translocation from the gut, which occurs when the gut barrier is compromised, leads to inflammation in the retina. Systemic treatment with antibiotics also prevented the onset and progression of ocular disease in *CRB1*-IRD models. A compromised gut barrier in *CRB1*-IRD patients might, through systemic inflammation, lead to complement activation, further implicating the role of the complement cascade in *CRB1*-IRDs.

Among the plasma proteins that were decreased in the plasma of *CRB1*-IRD patients was the extracellular protein MFAP4, which is ubiquitously expressed and plays a role in intracellular interactions and cell adhesion. Macrophages drive local immune responses in retinal degeneration,^{52,53} and MFAP4 loss affects macrophage differentiation in animal models.⁵⁴ The elevated plasma levels of ADAMTS1 detected in *CRB1*-IRD patients may be related to angiogenic responses due to the vascular impairment secondary to degenerative changes in the retina.^{55–58} The ADAMTS1 enzyme is an angiogenic matrix-modifying enzyme that is upregulated by proinflammatory conditions in the retinal pigment epithelium (RPE).⁵⁹ We also detected elevated levels of PROS1, a protein involved in the homeostasis of RPE. Whole-exome sequencing has previously identified homozygous pathogenic variants in the *PROS1* gene as causing retinal dystrophy in two unrelated families,⁶⁰ potentially disrupting the vitamin K-dependent activities of PROS1, leading to RPE degradation. Further investigation is needed to determine whether the elevated levels of PROS1 are caused by retinal damage or by other biological events involving PROS1.

While the plasma proteome may reflect inflammation at the retinal level, it may also be influenced by functional vari-

ants in complement factor coding genes. The *CRB1* gene is located on chromosome 1 immediately downstream of the *CFH* locus. SNPs in the *CFH* locus have been associated with several retinal conditions in which CFH/CFHR proteins were also altered, including AMD, central serous chorioretinopathy, and multifocal choroiditis,^{19–25} indicating that this locus could be an important disease-modifying locus for eye conditions.

Using TaqMan SNP genotyping technology, we found evidence for a skewed distribution of functional variants in the *CFH* gene, which may predispose to altered complement factor levels in *CRB1*-IRDs or obscure relevant disease associations with plasma proteins, as demonstrated by our work. The significant skewing of the common *CFH* variants across *CRB1* pathogenic variants in our Dutch cohort is likely the result of frequent consanguineous marriages in geographically more isolated populations, such as the strict geographical location of the p.(Met1041Thr) in the Netherlands, and predisposes to homozygosity of harmful recessive alleles. Genotype frequencies, Hardy–Weinberg equilibrium assumptions, and allele frequencies can be affected by relatedness, and our study demonstrates that addressing relatedness is crucial to ensure the accuracy of genotype–disease relationships and assessment of quantification of the complement factors in *CRB1*-IRDs and other family-based monogenic conditions. We believe this genetic “confounding” of common variants is currently strongly underappreciated in molecular profiling studies of *CRB1*-IRDs.

While we show that in a second global cohort, there is no association with the *CFH/CFHR* locus in *CRB1* cases in general, data from the well-powered UK Biobank demonstrated a linkage between variants in *CFH* and *CRB1*. Several key missense variants (e.g., p.(Cys948Tyr)) are nearly exclusively inherited with one of the two alleles of rs7535263, which tag functionally distinct *CFH/CFHR* haplotypes and predispose to altered composition of plasma complement factors.^{11,12} This linkage is expected from their proximity on the genome and LD signatures in the general population and has important implications for future research and treatment modalities: (1) Our study demonstrates that complement factor components are involved in *CRB1*-IRDs but that relative biological relatedness (i.e., founder effects) between individuals or linkage with functional variants in the *CFH* locus should be considered in follow-up studies of complement dysregulation in human studies of *CRB1*-IRDs. (2) While we demonstrate that correcting for the genotype of rs7535263 revealed an otherwise obscured increase in CFHR2 levels in patients, it is not unlikely that additional CFH(R) gene variants that genetically predispose to altered complement factor levels contribute to the pathophysiology of *CRB1*-IRDs. The limited sample size of our study and the lack of probing for other CFH-related factors encoded by genes upstream of the *CRB1* locus (e.g., *CFHR1* and *CFHR3* levels correlate with the genotype of rs7535263 according to *gtexportal*) may have resulted in an underestimation of the differences in the levels of complement factors in *CRB1*-IRD patients compared to controls. (3) Many more common variants in immune genes are likely involved in disease-modifying pathways that may influence the severity and disease course of *CRB1*-IRDs. The use of genome-wide association studies using well-defined clinical endpoints, preferably based on microperimetry,⁶¹ may aid in the discovery of these common variants and could improve genotype–phenotype correlations to better predict disease course and perhaps lead to therapeutic modalities that can

alter the disease course. The latter may also be of interest for emerging *CRB1* gene augmentation therapy or mutational correction by allelic substitution via CRISPR/Cas9-mediated homology-directed repair or base editing^{62,63} because these therapeutic approaches are accompanied by immune activation when administered intravitreally or subretinally.⁶⁴ It would be important to determine to what extent the inflammatory markers identified in this study may help understand the side effects of gene therapy, such as increased chorioretinal atrophy, which has recently been described after gene therapy using voretigene neparvovec for *RPE65*-associated retinal dystrophies.^{65,66} A major source of plasma complement components is the liver, but complement proteins are also produced and expressed in the retina, as well as by immune cells and various tissues. Complement activation may occur in the retina due to loss of tissue integrity caused by *CRB1* dysfunction, and modulating the complement system without addressing this primary cause may not have a clinically significant impact on the progression of the disease. Regardless, a complement-targeted therapy may be useful as a combination therapy to minimize adverse reactions from *CRB1* gene-correcting strategies in retinal degeneration and potentially even in other gene therapy strategies for IRDs. In future studies, it might be informative to determine the immune profile of patients before commencing gene therapy interventions to determine to what extent complement activation and plasma concentrations influence outcome in patients.

In conclusion, our results implicate the involvement of the complement cascade in *CRB1*-IRDs. For future research, gene association studies of all SNPs in the genome with a categorization of patients based on disease severity may provide more insight into the pathophysiology of *CRB1*-IRDs and IRDs in general.

Acknowledgments

The authors thank N.H. ten Dam-van Loon, J. Ossewaarde-van Norel, and V. Koopman-Kalinina Ayuso for their assistance performing slit-lamp examination and assessment of vitreous cells and vitreous haze on all included patients.

Supported by the Bartimeus Foundation (LM, JHdB, SH, AdL, XN, LlvdB, CB, MMvG, JJWK), VHRN vision health research network and FBC fighting blindness Canada (RK), and Swiss National Science Foundation (Grant 204285) and European Union (Grant EJP-RD19-234, Solve-Ret) (CR).

Disclosure: **L. Moekotte**, None; **J.H. de Boer**, None; **S. Hiddingh**, None; **A. de Ligt**, None; **X.-T.-A. Nguyen**, None; **C.B. Hoyng**, None; **C.F. Inglehearn**, None; **M. McKibbin**, None; **T.M. Lamey**, None; **J.A. Thompson**, None; **F.K. Chen**, None; **T.L. McLaren**, None; **A. AlTalishi**, None; **D.M. Panneman**, None; **E.G.M. Boonen**, None; **S. Banfi**, None; **B. Bocquet**, None; **I. Meunier**, None; **E. De Baere**, None; **R. Koenekoop**, None; **M. Oldak**, None; **C. Rivolta**, None; **L. Roberts**, None; **R. Ramesar**, None; **R. Strupaitė-Šileikienė**, None; **S. Kohl**, None; **G. Jane Farrar**, None; **M. van Vugt**, None; **J. van Setten**, None; **S. Roosing**, None; **L.I. van den Born**, None; **C.J.F. Boon**, None; **M.M. van Genderen**, None; **J.J.W. Kuiper**, None

References

1. Bujakowska K, Audo I, Mohand-Säid S, et al. *CRB1* mutations in inherited retinal dystrophies. *Hum Mutat*. 2012;33(2):306.

2. Den Hollander AI, Heckenlively JR, van den Born LI, et al. Leber congenital amaurosis and retinitis pigmentosa with Coats-like exudative vasculopathy are associated with mutations in the crumbs homologue 1 (CRB1) gene. *Am J Hum Genet.* 2001;69(1):198–203.
3. Den Hollander AI, Davis J, Van Der Velde-Visser SD, et al. CRB1 mutation spectrum in inherited retinal dystrophies. *Hum Mutat.* 2004;24(5):355–369.
4. Talib M, Van Cauwenbergh C, De Zaeytijd J, et al. CRB1-associated retinal dystrophies in a Belgian cohort: genetic characteristics and long-term clinical follow-up. *Br J Ophthalmol.* 2022;106(5):696–704.
5. Hettinga YM, van Genderen MM, Wieringa W, Ossewaarde-van Norel J, de Boer JH. Retinal dystrophy in 6 young patients who presented with intermediate uveitis. *Ophthalmology.* 2016;123(9):2043–2046.
6. Verhagen F, Kuiper J, Nierkens S, Imhof SM, Radstake T, de Boer J. Systemic inflammatory immune signatures in a patient with CRB1 linked retinal dystrophy. *Expert Rev Clin Immunol.* 2016;12(12):1359–1362.
7. Watson CM, El-Asrag M, Parry DA, et al. Mutation screening of retinal dystrophy patients by targeted capture from tagged pooled DNAs and next generation sequencing. *PLoS One.* 2014;9(8):e104281.
8. De Castro-Miró M, Pomares E, Lorés-Motta L, et al. Combined genetic and high-throughput strategies for molecular diagnosis of inherited retinal dystrophies. *PLoS One.* 2014;9(2):e88410.
9. Alves CH, Wijnholds J. Microglial cell dysfunction in CRB1-associated retinopathies. *Adv Exp Med Biol.* 2019;1185:159–163.
10. Moekotte L, Kuiper JJW, Hiddingh S, et al. CRB1-associated retinal dystrophy patients have expanded Lewis glycoantigen-positive T cells. *Invest Ophthalmol Vis Sci.* 2023;64(13):6.
11. Sun BB, Maranville JC, Peters JE, et al. Genomic atlas of the human plasma proteome. *Nature.* 2018;558(7708):73–79.
12. Emilsson V, Gudmundsson EF, Jonmundsson T, et al. A proteogenomic signature of age-related macular degeneration in blood. *Nat Commun.* 2022;13(1):3401.
13. Lynch AM, Wagner BD, Mandava N, et al. The relationship of novel plasma proteins in the early neonatal period with retinopathy of prematurity. *Invest Ophthalmol Vis Sci.* 2016;57(11):5076–5082.
14. Kuiper JJW, Verhagen FH, Hiddingh S, et al. A network of serum proteins predict the need for systemic immunomodulatory therapy at diagnosis in noninfectious uveitis. *Ophthalmol Sci.* 2022;2(3):100175.
15. Achten R, van Luijk C, Thijs J, et al. Non-infectious uveitis secondary to dupilumab treatment in atopic dermatitis patients shows a pro-inflammatory molecular profile. *Ocul Immunol Inflamm.* 2024;32(7):1150–1154.
16. Wennink RAW, Ayuso VK, Tao W, Delemarre EM, de Boer JH, Kuiper JJW. A blood protein signature stratifies clinical response to csDMARD therapy in pediatric uveitis. *Transl Vis Sci Technol.* 2022;11(2):4.
17. Wierenga APA, Cao J, Mouthaan H, et al. Aqueous humor biomarkers identify three prognostic groups in uveal melanoma. *Invest Ophthalmol Vis Sci.* 2019;60(14):4740–4747.
18. Haq Z, Yang D, Psaras C, Stewart JM. Sex-based analysis of potential inflammation-related protein biomarkers in the aqueous humor of patients with diabetes mellitus. *Transl Vis Sci Technol.* 2021;10(3):1–8.
19. Cipriani V, Lorés-Motta L, He F, et al. Increased circulating levels of Factor H-Related Protein 4 are strongly associated with age-related macular degeneration. *Nat Commun.* 2020;11(1):778.
20. Lorés-Motta L, van Beek AE, Willems E, et al. Common haplotypes at the CFH locus and low-frequency variants in CFHR2 and CFHR5 associate with systemic FHR concentrations and age-related macular degeneration. *Am J Hum Genet.* 2021;108(8):1367–1384.
21. denHollander AI, Mullins RF, Orozco LD, et al. Systems genomics in age-related macular degeneration. *Exp Eye Res.* 2022;225:109248.
22. Kaye R, Chandra S, Sheth J, Boon CJF, Sivaprasad S, Lotery A. Central serous chorioretinopathy: an update on risk factors, pathophysiology and imaging modalities. *Prog Retin Eye Res.* 2020;79:100865.
23. Schellevis RL, Van Dijk EHC, Breukink MB, et al. Role of the complement system in chronic central serous chorioretinopathy: a genome-wide association study. *JAMA Ophthalmol.* 2018;136(10):1128–1136.
24. de Groot EL, Ossewaarde-van Norel J, de Boer JH, et al. Association of risk variants in the CFH gene with elevated levels of coagulation and complement factors in idiopathic multifocal choroiditis. *JAMA Ophthalmol.* 2023;141(8):737–745.
25. Ferrara DC, Merriam JE, Freund KB, et al. Analysis of major alleles associated with age-related macular degeneration in patients with multifocal choroiditis: strong association with complement factor H. *Arch Ophthalmol.* 2008;126(11):1562–1566.
26. Ferkingstad E, Sulem P, Atlason BA, et al. Large-scale integration of the plasma proteome with genetics and disease. *Nat Genet.* 2021;53(12):1712–1721.
27. Machiela MJ, Chanock SJ. LDassoc: an online tool for interactively exploring genome-wide association study results and prioritizing variants for functional investigation. *Bioinformatics.* 2018;34(5):887–889.
28. Auton A, Abecasis GR, Altshuler DM, et al. A global reference for human genetic variation. *Nature.* 2015;526(7571):68–74.
29. Chang CC, Chow CC, Tellier LCAM, Vattikuti S, Purcell SM, Lee JJ. Second-generation PLINK: rising to the challenge of larger and richer datasets. *Gigascience.* 2015;4(1):7.
30. Hofmeister RJ, Ribeiro DM, Rubinacci S, Delaneau O. Accurate rare variant phasing of whole-genome and whole-exome sequencing data in the UK Biobank. *Nat Genet.* 2023;55(7):1243–1249.
31. Yeung MW, Wang S, Van De Vegte YJ, et al. Twenty-five novel loci for carotid intima-media thickness: a genome-wide association study in >45 000 individuals and meta-analysis of >100 000 individuals. *Arterioscler Thromb Vasc Biol.* 2022;42(4):484–501.
32. van Rheenen W, van der Spek RAA, Bakker MK, et al. Common and rare variant association analyses in amyotrophic lateral sclerosis identify 15 risk loci with distinct genetic architectures and neuron-specific biology. *Nat Genet.* 2021;53(12):1636–1648.
33. Panneman DM, Hitti-Malin RJ, Holtes LK, et al. Cost-effective sequence analysis of 113 genes in 1,192 probands with retinitis pigmentosa and Leber congenital amaurosis. *Front Cell Dev Biol.* 2023;11:1112270.
34. Nevola K, Sandin M, Guess J, et al. OlinkAnalyze: Facilitate Analysis of Proteomic Data from Olink. R package version 4.0.2. 2024; <https://github.com/olink-proteomics/olinkrpackage>.
35. Storey JD, Bass AJ, Dabney A, Robinson D. qvalue: Q-value estimation for false discovery rate control. R package version 2.38.0. <http://github.com/jdstorey/qvalue>.
36. Wu T, Hu E, Xu S, et al. clusterProfiler 4.0: A universal enrichment tool for interpreting omics data. *Innovation (Cambridge Mass).* 2021;2(3):100141.
37. Visualization of functional enrichment result | Biomedical Knowledge Mining using GOSemSim and clusterProfiler.

- Guangchuan Yu, Southern Medical University, <https://yulab-smu.top/biomedical-knowledge-mining-book/enrichplot.html>. Accessed April 4, 2023.
38. Wei T, Simko V. (2024). R package 'corrplot': visualization of a correlation matrix. (Version 0.95), <https://github.com/taiyun/corrplot>.
 39. Wickham H. (2016). ggplot2: elegant graphics for data analysis. New York: Springer-Verlag. ISBN 978-3-319-24277-4, <https://ggplot2.tidyverse.org>.
 40. Den Hollander AI, Ten Brink JB, De Kok YJM, et al. Mutations in a human homologue of Drosophila crumbs cause retinitis pigmentosa (RP12). *Nat Genet.* 1999;23(2):217–221.
 41. Kousal B, Dudakova L, Gaillyova R, et al. Phenotypic features of CRB1-associated early-onset severe retinal dystrophy and the different molecular approaches to identifying the disease-causing variants. *Graefes Arch Clin Exp Ophthalmol.* 2016;254(9):1833–1839.
 42. Lopes da Costa B, Kolesnikova M, Levi SR, et al. Clinical and therapeutic evaluation of the ten most prevalent CRB1 mutations. *Biomedicines.* 2023;11(2):385.
 43. Whaley K, Ruddy S. Modulation of C3b hemolytic activity by a plasma protein distinct from C3b inactivator. *Science.* 1976;193(4257):1011–1013.
 44. Eberhardt HU, Buhlmann D, Hortschansky P, et al. Human factor H-related protein 2 (CFHR2) regulates complement activation. *PLoS One.* 2013;8(11):e78617.
 45. Cipriani V, Tierney A, Griffiths JR, et al. Beyond factor H: The impact of genetic-risk variants for age-related macular degeneration on circulating factor-H-like 1 and factor-H-related protein concentrations. *Am J Hum Genet.* 2021;108(8):1385–1400.
 46. Cserhalmi M, Papp A, Brandus B, Uzonyi B, Józsi M. Regulation of regulators: role of the complement factor H-related proteins. *Semin Immunol.* 2019;45:101341.
 47. Silverman SM, Ma W, Wang X, Zhao L, Wong WT. C3- and CR3-dependent microglial clearance protects photoreceptors in retinitis pigmentosa. *J Exp Med.* 2019;216(8):1925–1943.
 48. Wang S, Du L, Yuan S, Peng GH. Complement C3a receptor inactivation attenuates retinal degeneration induced by oxidative damage. *Front Neurosci.* 2022;16:951491.
 49. Hoh Kam J, Lenassi E, Malik TH, Pickering MC, Jeffery G. Complement component C3 plays a critical role in protecting the aging retina in a murine model of age-related macular degeneration. *Am J Pathol.* 2013;183(2):480–492.
 50. Wykoff CC, Hershberger V, Eichenbaum D, et al. Inhibition of complement factor 3 in geographic atrophy with NGM621: phase 1 dose-escalation study results. *Am J Ophthalmol.* 2022;235:131–142.
 51. Peng S, Li JJ, Song W, et al. CRB1-associated retinal degeneration is dependent on bacterial translocation from the gut. *Cell.* 2024;187(6):1387–1401.e13.
 52. Yu C, Roubex C, Sennlaub F, Saban DR. Microglia versus monocytes: distinct roles in degenerative diseases of the retina. *Trends Neurosci.* 2020;43(6):433–449.
 53. Guo M, Schwartz TD, Dunaief JL, Cui QN. Myeloid cells in retinal and brain degeneration. *FEBS J.* 2022;289(8):2337–2361.
 54. Ong SLM, de Vos IJHM, Meroshini M, Poobalan Y, Dunn NR. Microfibril-associated glycoprotein 4 (Mfap4) regulates haematopoiesis in zebrafish. *Sci Rep.* 2020;10(1):11801.
 55. Rajabian F, Arrigo A, Bianco L, et al. Optical coherence tomography angiography in CRB1-associated retinal dystrophies. *J Clin Med.* 2023;12(3):1095.
 56. Murro V, Mucciolo DP, Sodi A, et al. Retinal capillaritis in a CRB1-associated retinal dystrophy. *Ophthalmic Genet.* 2017;38(6):555–558.
 57. Alonso F, Dong Y, Li L, et al. Fibrillin-1 regulates endothelial sprouting during angiogenesis. *Proc Natl Acad Sci USA.* 2023;120(23):e2221742120.
 58. Talib M, van Schooneveld MJ, van Genderen MM, et al. Genotypic and phenotypic characteristics of CRB1-associated retinal dystrophies: a long-term follow-up study. *Ophthalmology.* 2017;124(6):884–895.
 59. Bevirt DJ, Mohamed J, Catterall JB, et al. Expression of ADAMTS metalloproteinases in the retinal pigment epithelium derived cell line ARPE-19: transcriptional regulation by TNF α . *Biochim Biophys Acta.* 2003;1626(1–3):83–91.
 60. Bushehri A, Zare-Abdollahi D, Alavi A, Dehghani A, Mousavimikala M, Khorshid HRK. Identification of PROS1 as a novel candidate gene for juvenile retinitis pigmentosa. *Int J Mol Cell Med.* 2019;8(3):179–190.
 61. Nguyen XTA, Talib M, van Schooneveld MJ, et al. CRB1-associated retinal dystrophies: a prospective natural history study in anticipation of future clinical trials. *Am J Ophthalmol.* 2022;234:37–48.
 62. Boon N, Lu X, Andriessen CA, et al. AAV-mediated gene augmentation therapy of CRB1 patient-derived retinal organoids restores the histological and transcriptional retinal phenotype. *Stem Cell Reports.* 2023;18(5):1123–1137.
 63. da Costa BL, Li Y, Levi SR, Tsang SH, Quinn PMJ. Generation of CRB1 RP patient-derived iPSCs and a CRISPR/Cas9-mediated homology-directed repair strategy for the CRB1 c.2480G>T mutation. *Adv Exp Med Biol.* 2023;1415:571–576.
 64. Nguyen XTA, Moekotte L, Plomp AS, Bergen AA, van Genderen MM, Boon CJF. Retinitis pigmentosa: current clinical management and emerging therapies. *Int J Mol Sci.* 2023;24(8):7481.
 65. Gange WS, Sisk RA, Besirli CG, et al. Perifoveal chorioretinal atrophy after subretinal voretigene neparvovec-rzyl for RPE65-mediated leber congenital amaurosis. *Ophthalmol Retina.* 2022;6(1):58–64.
 66. Reichel FF, Seitz I, Wozar F, et al. Development of retinal atrophy after subretinal gene therapy with voretigene neparvovec. *Br J Ophthalmol.* 2023;107(9):1331–1335.